Title

Dynamic Time-Resolved Fluorescence Lifetime Measurements in situ Using a Dip Probe

ISBN

9798293834860

Author

Coffey, Lia Aranda

Publication Date

2025-09-12

Peer reviewed|Thesis/dissertation

UNIVERSITY OF CALIFORNIA

Los Angeles

Dynamic Time-Resolved Fluorescence Lifetime Measurements *in situ* Using a Dip Probe

A dissertation submitted in partial satisfaction of the

requirements for the degree Master of Science

in Chemistry

by

Lia Aranda Coffey

2025

ABSTRACT OF THE DISSERTATION

Dynamic Time-Resolved Fluorescence Lifetime

Measurements *in situ* Using a Dip Probe

by

Lia Aranda Coffey

University of California, Los Angeles, 2025

Professor Justin Ryan Caram, Chair

Abstract

This thesis establishes a fiber-based dip probe method for *in situ* time correlated single photon counting (TCSPC), enabling real time photoluminescent lifetime monitoring in dynamic chemical system without disrupting the native sample environment.[1] Unlike intensity-based measurements, which depend on experimental conditions, luminescent lifetimes are ratiometric, intrinsic to the excited state, and provide direct insight to sample photophysical properties that are directly linked to local environment changes.[1–3] By integrating a fiber optic probe with TCSPC, lifetimes can be directly monitored in experimental chemistry environments that have otherwise been inaccessible, extending the reach of photoluminescent lifetime spectroscopy beyond current, conventional tabletop, cuvette based optical setups. In addition to *in situ* monitoring, the dip probe method allows for rapid sequential lifetime measurements across multiple samples with minimal maintenance of the system, allowing for more automated, high-

throughput measurements of luminescent properties. These methods are demonstrated across four systems: sequential lifetime measurements of synthetic dyes, Rhodamine 6G and 3,3′-bis(2-sulfopropyl)-5,5′,6,6′-tetrachloro-1,1′-dioctylbenzimidacarbocyanine (C8S3) monomer, and dynamic studies of ultrasmall Mercury Telluride (HgTe) quantum dot synthesis, as well as J-aggregation of both C8S3 ribbons and double-walled nanotubes (DWNTs). These chemical systems establish the dip probe as a versatile platform for probing excited-state dynamics *in situ*, while also providing a practical, high-throughput route for consecutive lifetime measurements.

The thesis of Lia Aranda Coffey is approved.

Victoria Barber

Benjamin Joel Schwartz

Justin Ryan Caram, Committee Chair

University of California, Los Angeles

2025

Table of Contents

Acknowledgements

The four years prior to this one have brought significant personal challenges that weighed heavily on my life. When I began my first quarter in this program, I struggled with motivation and often felt uncertain about continuing. Initially, the only motivation that pushed me forward was the understanding that this was an opportunity I could not take for granted.

The way my life has turned around is truly shocking, and it fills my heart with gratitude. I could have never imagined that my time in this program would bring back my excitement for both life and chemistry. I am deeply thankful for all the opportunities I've received this year that have allowed me to learn and grow in so many areas of life.

Firstly, I would like to thank my mentor, Ash Hua, and my assistant mentor, Anthony Sica, for always leading me toward deeper knowledge and understanding of novel spectroscopy. I would also like to thank Belle Coffey, Arthur Odenheimer, Lexi Wright, Elijah Cook, Caleb Pike, Richard Liu, and Anneka Miller Casas for creating an encouraging group environment that allowed me to explore and learn so much diverse chemistry.

I would like to thank Dr. Justin Caram for always being a supportive leader and a good person to our group. I would also like to thank Dr. Sarah Tolbert for reminding me of the childlike wonder that comes with doing chemistry. I am grateful as well to Dr. Benjamin Schwartz and Dr. Victoria Barber for their guidance and thoughtful review of this dissertation.

Lastly, with my whole heart, I would like to thank my friends and family for always being there to help me through it all.

Chapter 1: Introduction

1.1 Overview

This research expands the reach of time-correlated single photon counting (TCSPC) by developing a fiber-based dip probe for *in situ* lifetime measurements. Conventional TCSPC lifetime spectroscopy is typically done in cuvettes, or via microscope, limiting its applications in dynamic chemical systems, which may require special handling outside of a laser lab. In such systems, real-time monitoring could enable unique insight into reactivity and high-throughput screening. By directly immersing the probe into reaction environments, this method enables noninvasive, high-resolution tracking of excited-state dynamics during reaction conditions, or in a high throughput manner. The ability to monitor lifetimes, an intrinsic, ratiometric property of chromophores, offers an opportunity to study photophysical changes such as aggregation, defect formation, or nanocrystal growth that remain hidden. Beyond providing new insight into fundamental processes, the dip probe format facilitates rapid, sequential measurements across multiple samples, positioning it as a scalable approach for high-throughput photophysical screening. This method actively bridges the gap between controlled optical experiments and real-world chemical environments.

1.2 Luminescence and Lifetimes

When light with sufficiently high energy interacts with a chemical system, a molecule can absorb a photon and transition from the electronic ground state to an electronic excited state. The electron will remain in the excited state for a short amount of time, losing energy through vibrations as it relaxes to the potential energy minima of the excited state. The chemical system can then relax to its ground state via emission of a photon, with the energy difference between

absorption and emission termed a Stokes shift. This phenomenon is called luminescence, which generally includes both fluorescence and phosphorescence.[2]

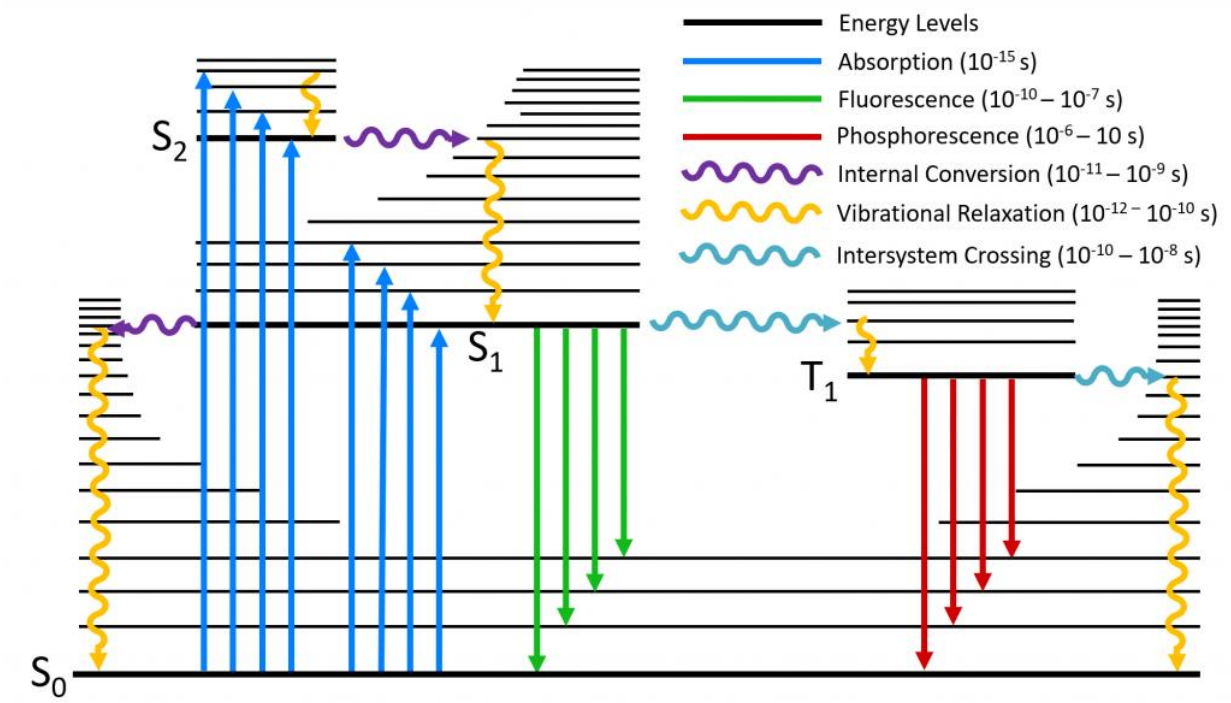

Figure 1. Jablonski diagram depicting the following photophysical events: absorption, fluorescence, phosphorescence, internal conversion, vibrational relaxation, and intersystem crossing, as well as their relative timescales.[2,4]

Fluorescence is the luminescence process that occurs when a molecule emits light upon transition from the singlet excited state (S_1) to the singlet ground state (S_0). As this does not involve a spin flip, fluorescent lifetimes tend to be short ranging from picoseconds to nanoseconds in length.[2] Phosphorescence occurs when the initial singlet excited state undergoes intersystem crossing into the triplet state (T_1) before relaxing back down to the ground state. The excited electron has the same spin leftover state preventing direct recombination and emission of a photon. This results in longer phosphorescent lifetimes ranging from microseconds to seconds. Both types of luminescent events and adjacent processes are expressed in Figure 1 with a Jablonski diagram. In addition, nonradiative pathways can deactivate the excited state back to the ground state, either via intersystem crossing or direct internal conversion.

A luminescent lifetime is a measure of the timescale of excited state deactivation via all processes, radiative and nonradiative. A monexponential decay law is shown below:

$$I(t) = I_0 e^{-t/\tau}$$

For this decay, the lifetime (τ) can be broken down into radiative and nonradiative parts, which cannot be directly separated without an additional measurement:

$$\tau = \frac{1}{k_{exp}} = \frac{1}{k_r + k_{nr} + k_{ISC}}$$

Separating radiative and nonradiative rates requires an estimate of the total quantum yield (Φ) of a chemical species upon excitation and is defined as the number of emitted photons relative to the number of absorbed photons as well as the equation below:

$$\Phi = \frac{photons\ emitted}{photons\ absorbed} = \frac{k_r}{k_r + k_{nr}}$$

Species with the highest photon conversion and little energy loss to vibrations have higher quantum yields and brighter emissions. In other words, high efficiency fluorophores have a large radiative to nonradiative decay ratio, implying that most of the particles of the species emit light upon relaxation. Fluorescent lifetimes and quantum yields are related through radiative and nonradiative decay constants. By relating the equations above, the following formula is obtained:

$$k_r = \frac{\Phi}{\tau}$$

This relationship allows for a full break down of excited state dynamics: separation of radiative and nonradiative rates.[2,3]

While luminescence intensity depends strongly on experimental variables such as concentration, path length, optical alignment, and excitation power, the luminescent lifetime is an intrinsic property of the excited state. It does not depend on the intensity of excitation or the

number of chromophores and is only affected by factors like the type of chromophore and local environments, making it a ratiometric observable.[2] While intensity can fluctuate due to changes in sample preparation or optical geometry, the lifetime remains stable under those conditions and varies only when the underlying excited state dynamics change. As a result, luminescent lifetimes provide a thorough and concentration independent insight of the chemical process' photophysical environment, making lifetimes valuable for detecting processes such as defect formation, aggregation, or quenching that may be hidden in steady state measurements.

1.3 Time Correlated Single Photon Counting

The fluorescence spectra can be measured via continuous light source (lamp or laser) which can resolve the intensity emission over a timescale far longer than the excited state. Time resolved photoluminescence measurements are less common but provide more information about the chemical species' dynamics and quenching as they measure how long a fluorophore stays in the exited state, requiring a pulsed excitation source. This work focuses on time correlated single photon counting (TCSPC) as method to measure fluorescent lifetimes. TCSPC leverages a pulsed laser, a single photon counting detector and a time-tagger electronic counter to measure photoluminescent lifetimes in picosecond time resolution; recording the time delay between an excitation pulse and the arrival time of an emitted photon.[1] There are two types of TCSPC lifetime acquisition methods utilized in this work: histogram mode, which bins photon events by their arrival time relative to the excitation, and time-tagged time-resolved mode that records each individual photon with both its relative arrival time and its absolute arrival time within the full experiment.[1] The time-tagged results can be reduced to a histogram, but also enable observation of lifetime dynamics while keeping track of the global experiment time. This method becomes more useful when applied to *in situ* probe measurements as it provides insight to real

photophysical impacts of dynamic processes such as nanocrystal growth or monomer aggregation directly in the solution environment. Here, a dip probe will be used to obtain these measurements as a means of direct system dynamics observation.

1.4 *In Situ* Measurements with a Dip Probe

A dip probe is fiber-optic device that is used to direct an excitation source into a sample and collect the resulting emission at the same tip via optical fibers.[5] This arrangement eliminates the need for tedious free-space alignment, allowing optical measurements to be made directly within a sealed or otherwise inaccessible environment. The compact geometry of the probe also makes it adaptable to reaction vessels, gloveboxes, or fume hoods where traditional optical setups are not possible.

While prior work has shown optical fibers can be used for *in situ* absorption and fluorescence measurements, only one report has suggested utility for liftetimes.[6] Early work demonstrated that TCSPC can be coupled to fibers, establishing that picosecond time resolution can be maintained even when excitation and emission are routed remotely.[1] These demonstrations confirmed that photoluminescent lifetimes, not just intensities, can be captured reliably through fiber optics. Fiber optic probes have been applied in biomedical contexts for fluorescence and Raman spectroscopy.[7,8] Thus fiber probes function reliably in complex, real-world environments such as living tissue, where conventional free-space optics are impractical, delivering and collecting light efficiently outside of the conditions of an optical table. However, prior work did not leverage commercial chemically resistant and high-temperature fiber probes suitable for the harsh environments that come with wet-chemical reactions.

For the most part, lifetime measurements have remained tied to cuvettes, flow cells, or other holders that require transferring material to a laser lab. While these arrangements are

acceptable for simple photophysical studies, they are poorly suited for studies of hazardous materials. Furthermore, interrupting chemistry to move aliquots into cuvettes could perturb the system of interest. This is especially limiting because changes in fluorescent lifetimes are the most direct indicators of local environmental changes, including reaction progression, self-assembly, and defect formation: processes that can remain hidden in steady-state absorption or emission spectra.

The dip probe method developed in this work addresses these challenges. By immersing the probe directly into the reaction medium, it enables true *in situ* lifetime monitoring of dynamic processes under realistic conditions. This makes the probe uniquely suited for environments where conventional setups are impractical, including flasks under stirring, glove boxes, and fume hoods. Beyond access, the dip probe also enables rapid sequential sampling of lifetimes without physically moving the sample, opening opportunities for automated, high-throughput studies of fluorescent properties. In doing so, it extends the advantages of time-resolved spectroscopy into settings that have previously been inaccessible.

1.5 Dip Probe Optical Setup

A 532 nm pulsed diode laser (PicoQuant, LDH-P-FA-530B) was directly coupled into the excitation fiber of a Visible-NIR reflection/backscatter probe (OceanOptics, QR400-7-VIS-NIR). The probe was submerged in the sample where the excitation events occur, and emitted light was collected back into the probe. The emission fiber was outcoupled into a free space set up where any lingering excitation light was filtered and the emission beam was focused onto a free space Avalanche photodiode detector (APD) (Micro Photon Devices, Photon Detecting Module). A pulsed laser driver (PicoQuant, PLD 800D) used an 80 MHz crystal oscillator to direct the repetition rate of the laser and acted as a time reference to all hardware. Both the laser driver and

detector communicated to the TCSPC timing module (PicoQuant, HydraHarp 400) to relate the photon events with respect to both microtime of the laser pulse and macrotime of the experiment. The optical layout of this method is shown in Figure 2 and the instrument response function (IRF) of the 532 nm pulsed diode laser was taken in whole milk a full width half maximum (FWHM) value of 108 ps and is shown in Figure 3.

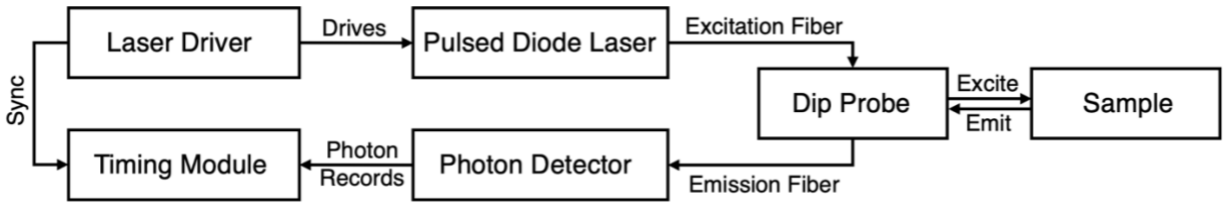

Figure 2. Schematic of dip probe optical setup.

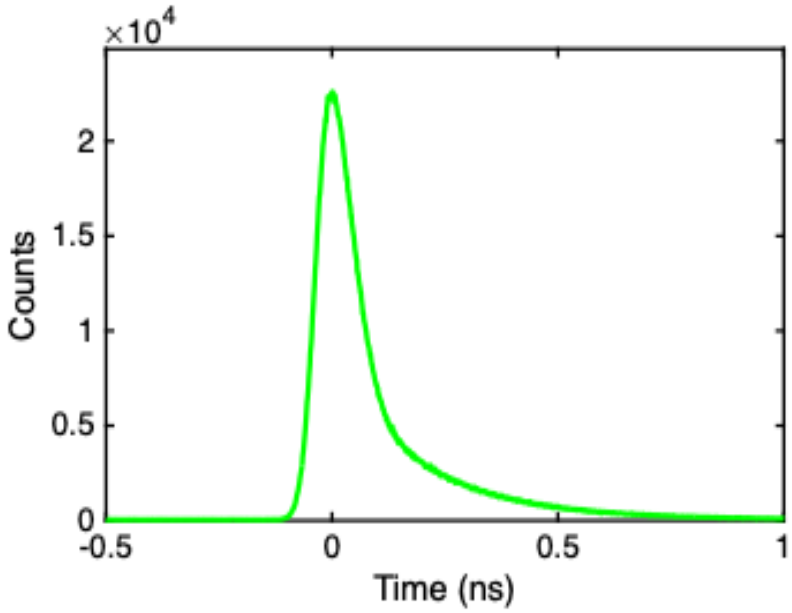

Figure 3. IRF of 532 nm pulsed laser. The full width half maximum (FWHM) value of this function was calculated to be 108 ps.

Chapter 2: Results and Discussion

2.1 Back-to-Back Lifetime Measurements

This work addresses common shortcomings of conventional TCSPC optical setups in maintenance, accessibility, and efficacy of multiple sample rotations by developing a means of conducting consecutive lifetime measurements via a fiber optic dip probe. To demonstrate the full capabilities of this novel method, lifetime measurements of two synthetic dyes, C8S3 monomer and Rhodamine 6G were taken in rapid succession of each other. The measurements were obtained by submerging the clean dip probe in the C8S3 monomer, collecting lifetime data, removing and cleaning the probe, and submerging it in Rhodamine 6G for the next round of data acquisition (Figures 4a, 4b, 4c). The cleaning and transfer of the dip probe between samples was a sub-thirty-second process. The timing module software in Figure 4 depicts two distinct fluorescent decays. The fluorescent lifetime for both the xanthine dye was found to be 3.8 ns, agreeing with the accepted literature values of around 4. [9,10] The plot of Rhodamine 6G lifetime decay obtained by the dip probe method is given in Figure 5.

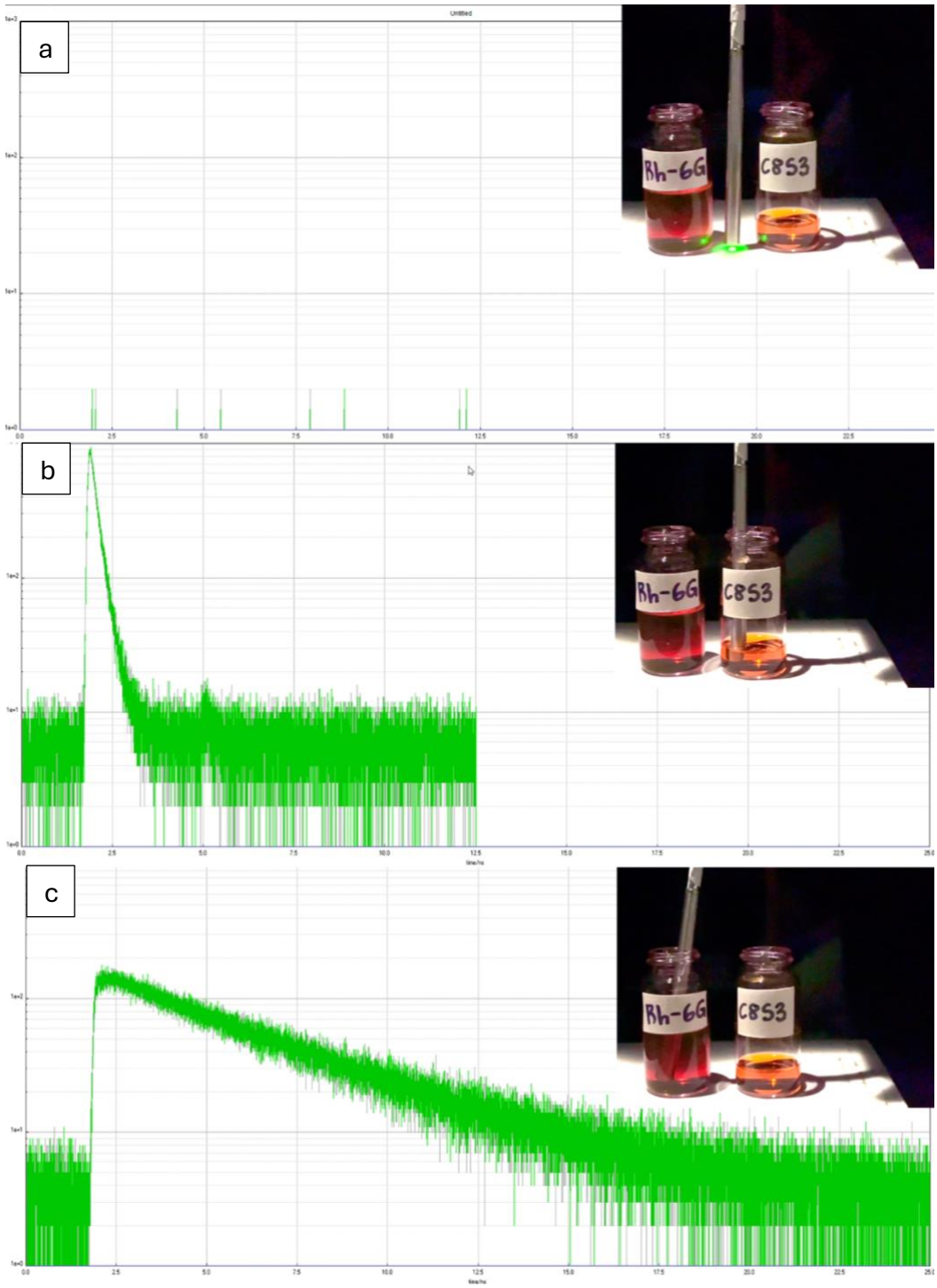

Figure 4. Successive lifetime measurements of C8S3 amphiphilic cyanine dye and Rhodamine 6G. 3 screenshots taken from a sub-five-minute video demonstrating (a) side-by-side vials with visible 532 nm beam sourced by dip probe, (b) a two-minute lifetime measurement of a C8S3 monomer followed by (c) a two-minute lifetime measurement of Rhodamine 6G, with a sub-30 second transition between measurements for preparing and cleaning the probe.

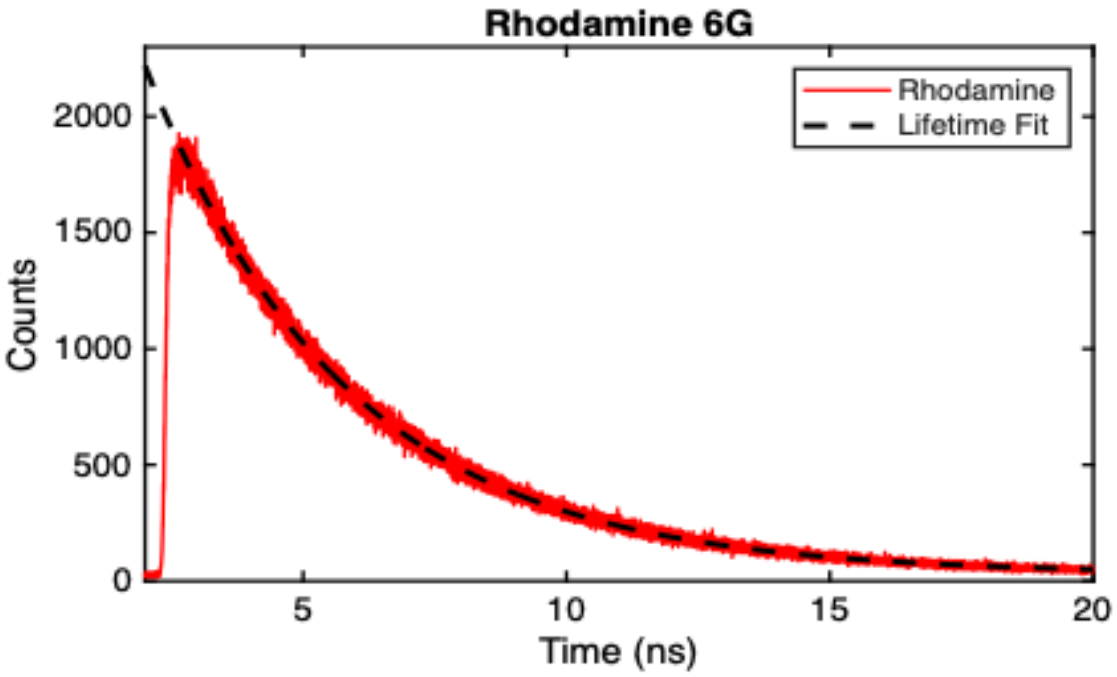

Figure 5. Fluorescent lifetime measurement of Rhodamine 6G taken with *in situ* dip probe. The red plot represents the recorded data while the dotted line shows the monexponential decay fit. The fit found $\tau = 3.8$ ns.

2.2 Mercury Telluride Quantum Dots

2.2.1 Nanocrystal Optical Properties

Quantum confinement occurs when semiconducting nanoparticles are comparable in size to the exciton Bohr radius, the size of the electron hole-pair in the bulk semiconductor. This forces the electron and hole wavefunctions to colocalize into a zero-dimension geometry, causing the electronic density of states to become discrete, shown in Figure 6.[11,12] Since the bandgap changes inversely with diameter, varying quantum dot size allows for tunable optical properties with absorption and emission shifting inversely with particle diameter.[13]

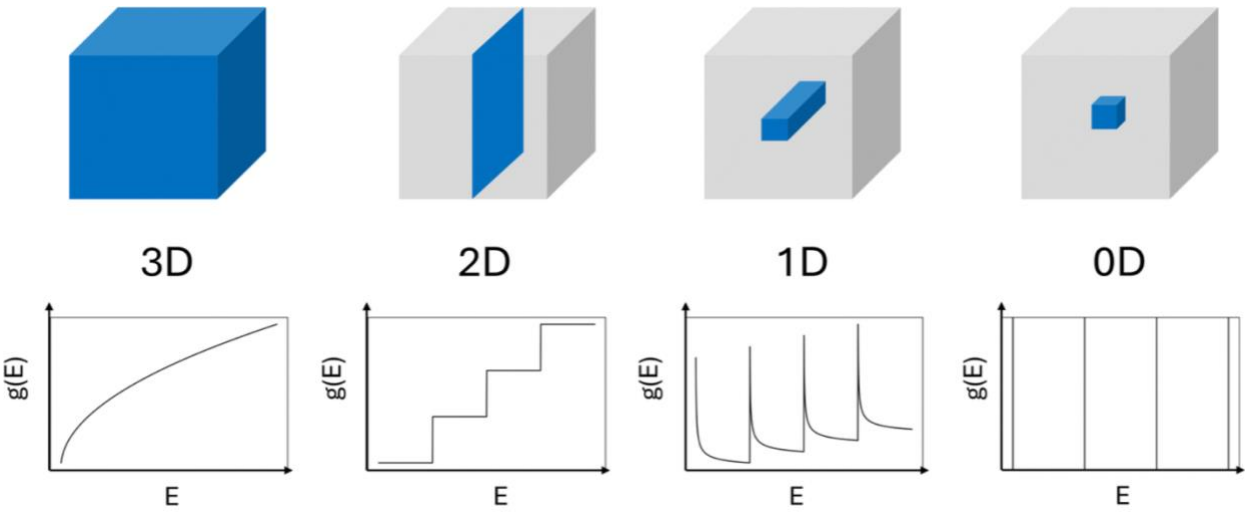

Figure 6. Density of states function (g(E)) transition from continuous bulk, to sheet, to wire, to discrete dot.[11,14]

2.2.2 HgTe Dot Synthesis

The in-situ dip probe method was tested on ultra small mercury telluride (HgTe) quantum dots. They were recently synthesized through a cold injection synthesis method and are of the smallest HgTe quantum dots recorded to date. The dots exhibit extreme quantum confinement at diameters of 1.7-2.3 nm that allow for tunable emission in the near to short wave infrared (NIR-SWIR) wavelengths (915-1180 nm). With a quantum yield of 80-90% in solution, the nanocrystal synthesis serves as an exceptional sample to study excited state dynamics as the dots nucleate and grow.

The HgTe quantum dot synthesis reaction was conducted under ambient atmosphere. 0.210 g of mercury (II) acetate was dissolved in 10.0 mL of oleylamine with mild heating until fully dissolved, then cooled to room temperature. Tellurium powder (250 mg) was dissolved in 2.0 mL n-trioctylphosphine to produce a clear yellow solution. The resulting 1.0 M TOPTe stock solution was diluted with tetrachloroethylene (TCE) to yield a 0.50 M TOPTe. 0.380 mL of this tellurium precursor solution was rapidly injected into the mercury acetate in oleylamine solution.

The solution immediately turned brown, indicating nucleation of HgTe QDs. The reaction was allowed to run for 1 hour while being monitored by the dip probe setup. A UV-vis was taken upon completion of the reaction to determine the extent of the quantum dot growth, showing a large species absorption peak at 910 nm and a smaller species absorption peak at 690 nm (Figure 7a, 7b, 7c).

2.2.3 Lifetime Dynamics of HgTe Quantum Dots

This work demonstrated the ability of the dip probe method to directly observe reaction dynamics in native environments without disrupting natural reaction progression or risking excessive human exposure to toxic chemicals in the process of aliquoting and preparing samples for standard TCSPC lifetime measurements. The synthesis of HgTe QDs was an optimal reaction to observe via this method. Firstly, the dip probe being inserted directly into the reaction solution limited direct contact with the extremely toxic mercury contents. Additionally, the requirement of continuous stirring of the reaction in a round-bottom flask was able to proceed uninterrupted throughout the progression of the experiment due to lack of aliquoting. Both of these contributions allowed the native environment of the reaction to remain undisturbed while the dynamics of the synthesis could be observed directly.

The reaction can be characterized by multiple distinct processes: nucleation, early growth, and surface passivation and stabilization. Nucleation lifetimes of the 690 nm absorbance dots population (Figure 7b) begin at 30 ns at the immediate start of the reaction, while the early growth phase was observed to show a sharp increase in lifetimes up to 80 ns at around 10 minutes of reaction time. Subsequent surface passivation and stabilization phases were observed to have a slight but steady decrease in lifetimes from 80 ns to 76 ns until the end of the reaction at 65 minutes (Figure 7c). The smooth lifetime measurements imply low defect formation in this

population. The large species population at 910 nm absorbance was out of range for available detectors.

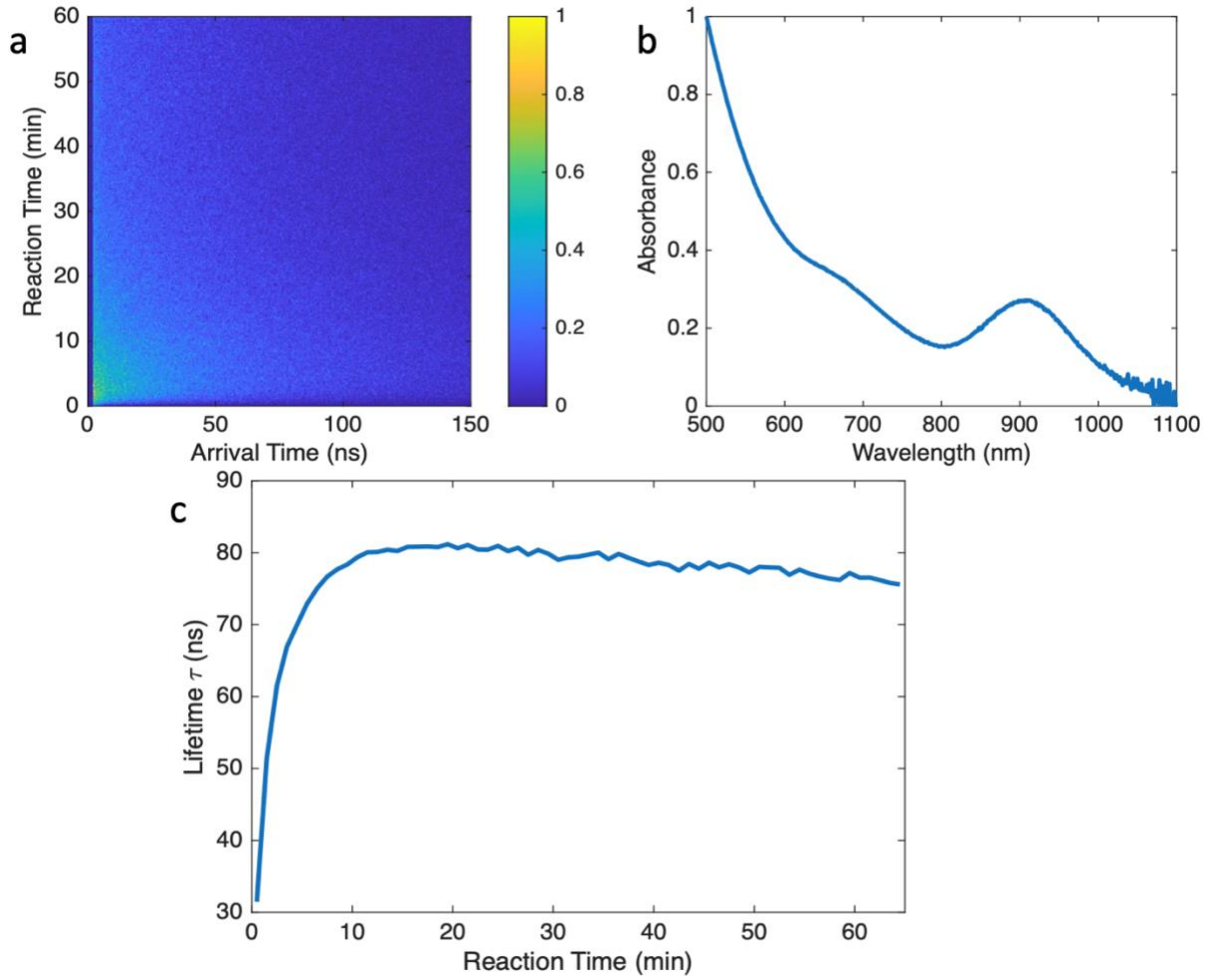

Figure 7. HgTe quantum dot (a) color map, normalized to power intensity, depicting photon record arrival times over the course of nanocrystal synthesis, (b) absorption spectra upon reaction completion, and (c) lifetime progression at 60-second intervals over full course of reaction (65 minutes).

2.3 C8S3 J-Aggregates

2.3.1 Aggregation and Excitons

An aggregate is the result of organic dye molecules, known as chromophores or monomers, self-assembling into supramolecular structures through noncovalent interactions such

as π-π stacking, electrostatic, or amphiphilic interactions.[15] When monomers aggregate, their electronic states are no longer confined to individual monomers; instead, the excitation can delocalize across multiple chromophores as a connected electron hole pair, known as a Frenkel exciton.[12,16] Excitons are the fundamental quasiparticles responsible for the shift in optical properties in aggregates.[16] Aggregates are characterized by the different types of monomer packing conformations of transition dipoles that form different types of delocalized excitonic states.

According to Kasha's model, there are three major types of aggregates that arise from these different packing arrangements: J, H, and X, that depend on head to tail, face to face, or orthogonal/crossed conformations, respectively.[15] Aggregation induced emission (AIE) happens under twisted conformations, but is not described by exciton coupling.

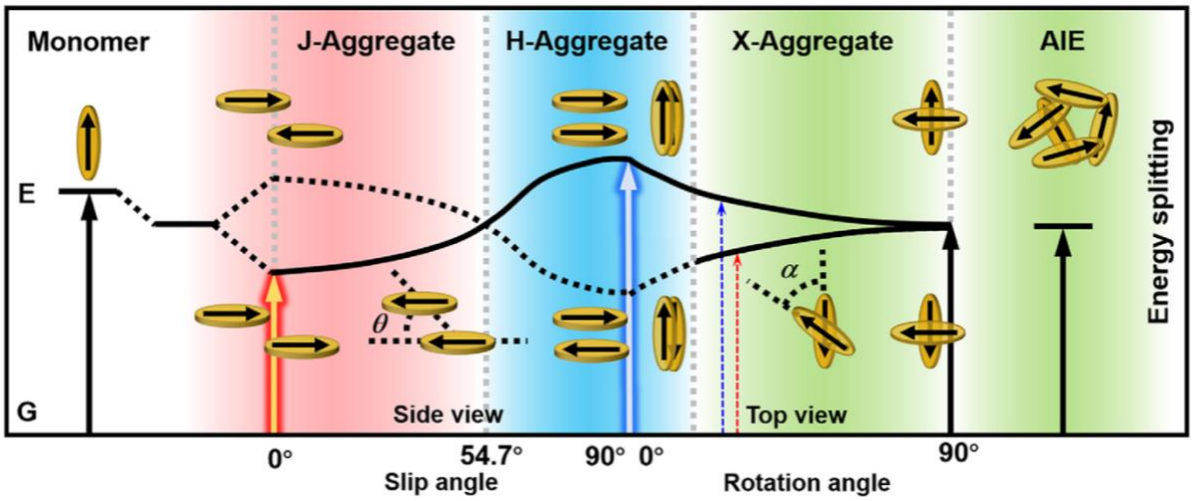

Figure 8. Different types of excited states and splitting based on aggregate type.[15,17]

Coupling of transition dipoles in J- and H-aggregates leads to excitonic energy level splitting. In J-aggregates, constructive dipole-dipole coupling makes the lowest exciton state optically allowed, producing red-shifted absorption and bright emission. In contrast, H-aggregates provide destructive coupling where the lowest exciton is dark; absorption is majorly blue-shifted and fluorescence is quenched due to the optically unavailable state.[15,17] This work

focuses on bright J-aggregates, whose strong radiative emission is particularly well-suited for TCSPC measurements.

Amphiphilic cyanine dyes are unique because they contain both hydrophobic alkyl chains and hydrophilic sulfonate groups that drive self-assembly in aqueous environments. Depending on how the transition dipoles in the chains couple during aggregation, 3,3′-bis(2-sulfopropyl)-5,5′,6,6′-tetrachloro-1,1′-dioctylbenzimidacarbocyanine (C8S3) monomers can aggregate into either blue shifted H-aggregates (deconstructive) or red shifted J-aggregates (constructive). In J-aggregates, constructive dipole-dipole interactions produce delocalized excitons upon excitation. This enhances the collective transition dipole moment and enables superradiant emission. In this work, the photophysical dynamics of the C8S3 J-aggregation of ribbons and more famously, doubled walled nanotubes (DWNTs) are examined.

Although ribbons and DWNTs are two different morphologies of C8S3 J-aggregates, they are also related. Crystallographic modeling of tube end geometry has shown that ribbons act as a precursor to the DWNT structure: flat 2D ribbons participate in helical winding to create the DWNT shape.[18] Since ribbons represent an earlier stage of nanotube formation, it is expected that excitons in ribbons are more localized in the 2D lattice and exhibit weaker radiative rates. The lifetime dynamic of both C8S3 J-aggregate ribbons and DWNTs are explored in this work.

2.3.2 J-Aggregation Induction Protocol

C8S3 dye (FEW Chemicals, S0440) was assembled into J-aggregates following the established “alcoholic route,” where dilution of a methanolic stock solution with water induces supramolecular aggregation. A monomer stock solution was first prepared by dissolving C8S3 in methanol (Fisher Chemicals, 99.9%) to a concentration of 1.5 mM. To initiate aggregation, 10.5 mL of purified water (Milli-Q, 18.2 MΩ·cm) was rapidly added to 4.5 μL of the C8S3 stock

solution under ambient conditions. The final mixture corresponded to a 30:70 methanol-to-water (v/v) ratio, which is known to promote the formation of extended J-aggregate nanostructures. Solutions were gently mixed by pipette inversion and allowed aggregate over a period of 3 hours. To ensure C8S3 ribbon formation, the solution was vigorously stirred during the aggregation period. DWNT aggregation was guaranteed by complete lack of stirring of the solution. A UV-vis was taken upon completion of the aggregation period to determine morphology of the C8S3 aggregates (Figure 9).[19]

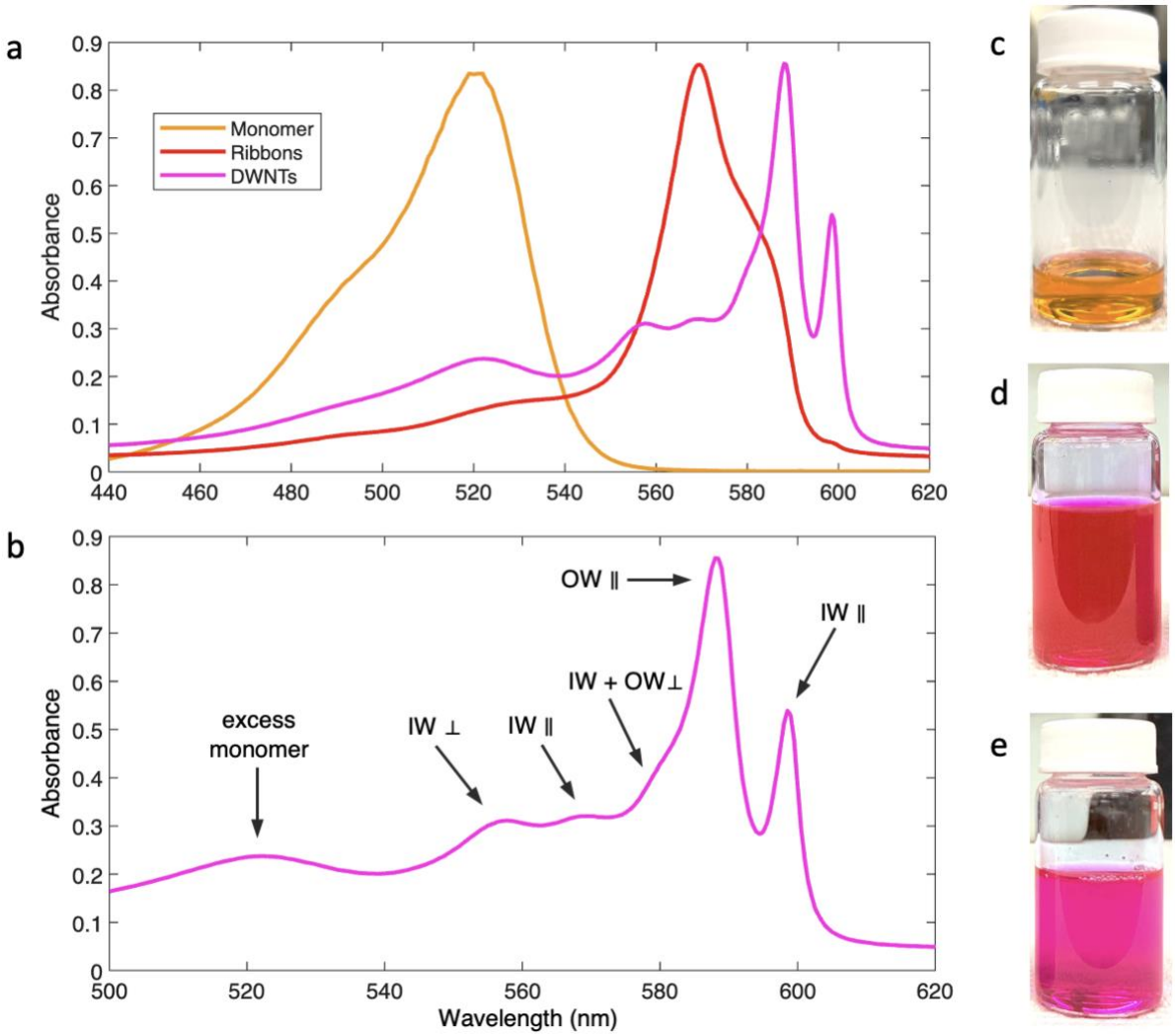

Figure 9. Absorbance spectra and sample pictures of various C8S3 morphologies. (a) Absorbance spectra of C8S3 monomer (orange), ribbons (red), and double-walled nanotubes (magenta). (b) Zoomed-in isolated spectrum of double-walled nanotubes with excitonic peak

labeling, and sample pictures of (c) monomer, (d) ribbon, and (e) double-walled nanotube morphologies.

2.3.3 Morphology Confirmation

The absorbance spectrum of the C8S3 double-walled nanotubes has multiple sharp peaks, which directly reflect the way the dye molecules arrange into the two cylindrical walls. In the monomer state, C8S3 absorbs broadly around 520 nm, but once the molecules assemble into nanotubes this feature splits into several distinct resonances that can be assigned according to wall (inner or outer) and dipole orientation (parallel or perpendicular) relative to the tube axis.[18,20,21] A strong, narrow band near 588 nm is attributed to the outer wall parallel transition, where excitons are delocalized along the tube axis in the outer cylinder. A second peak, slightly more red-shifted at 598 nm, is assigned to the inner wall parallel transition, which is shifted because of the tighter curvature and denser packing of the inner cylinder. In addition, the spectrum contains features corresponding to perpendicular transitions, where the transition dipoles oscillate around the tube. The inner wall perpendicular transition and the outer wall perpendicular transition appear as one resonance, a shoulder at 580 nm, reflecting overlap of the two. The narrowness and clear separation of these peaks are signatures of strong excitonic coupling and delocalization, and the presence of multiple distinct resonances demonstrates how both walls, and both orientations of excitonic dipoles, contribute separately to the overall optical response of the nanotubes.

By contrast, the absorbance spectrum of the C8S3 ribbon aggregates appears broader and less structured. In this morphology, the dye molecules pack into extended, flat, sheet-like arrangements as opposed to curved cylinders.[20] The main J-band of the ribbons is still red-shifted compared to the monomer, at 570 nm, which shows that J-type excitonic coupling is present. However, the peak is wider and not cleanly split, indicating that excitons are not as strongly

delocalized as in the nanotube morphology. The absence of two distinct J-bands highlights that ribbons lack the curvature-driven differentiation found in nanotubes; instead, their optical response is dominated by a single broad J-band, consistent with 2D sheet-like packing.

2.3.4 Lifetime Dynamics of C8S3 Aggregates

Observing aggregation processes is another key application for the dip probe method of tracking dynamics without disrupting the native environment. Aggregation is highly sensitive to environmental changes as it relies on non-covalent forces to hold monomers together. As such, any disturbance in the environment, including scientifically 'necessary' interruptions, such as taking aliquots, could heavily impact the aggregation process. Continuous mapping of average photon arrival times throughout the aggregation process is thus an important new tool in observing dynamics in these experiments.

The following photophysical measurements were able to be made using the time-tagged histogram mode of TCSPC to keep track of not only the photon arrival time of the records, but also the time in the 3-hour aggregation at which they arrived; these data are represented in the color map plot of Figure 10a and 11a. Using the same data, the photon arrival time was able to be calculated and averaged in chucks of photon records; these calculations were then related back to the overall aggregation time, as shown in Figures 10b and 11b.

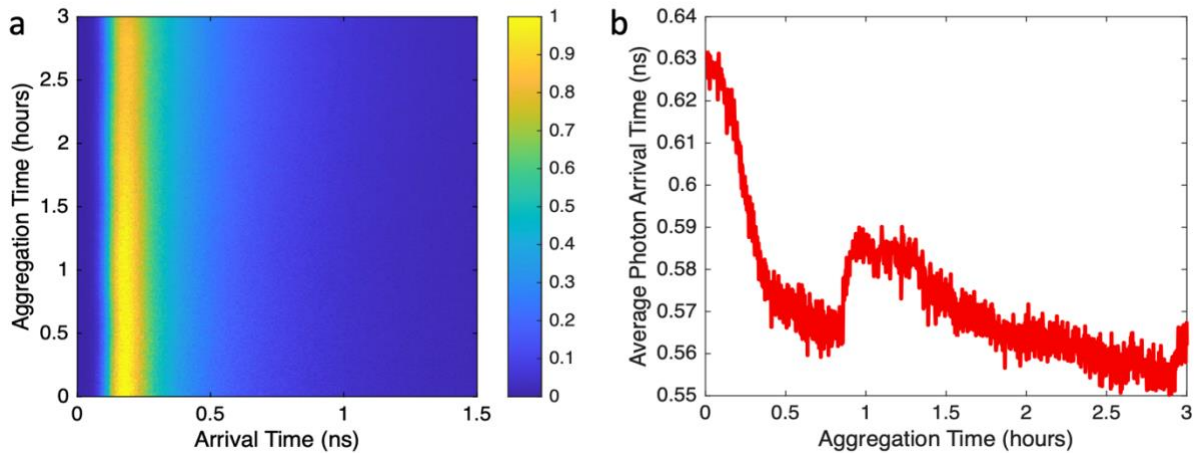

Figure 10. Time-tagged histogram records of C8S3 ribbons. (a) Color map, normalized to power intensity, depicting photon record arrival times over the course of C8S3 aggregation. (b) Average photon arrival time over course of 3-hour aggregation.

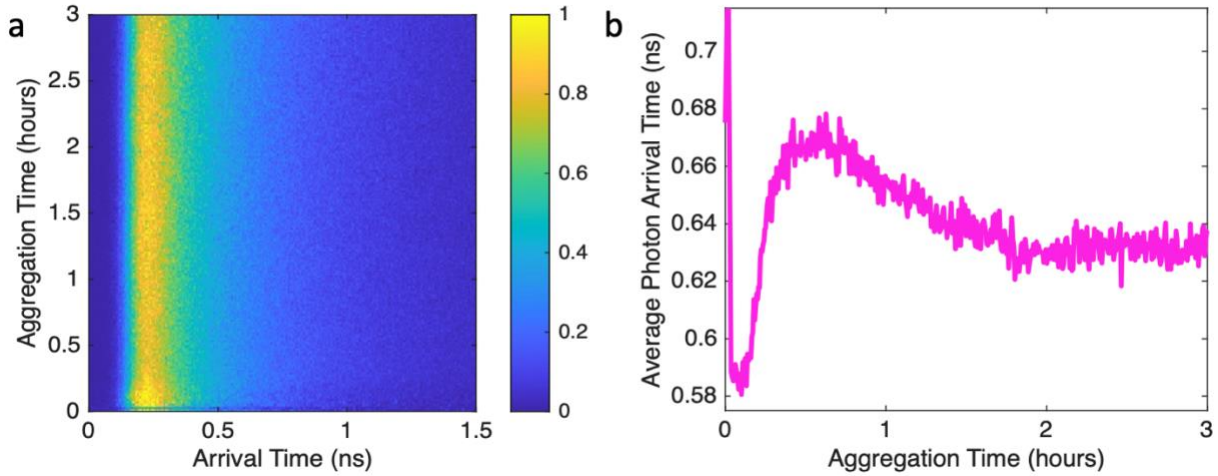

Figure 11. Time-tagged histogram records of C8S3 double-walled nanotubes. (a) Color map, normalized to power intensity, depicting photon record arrival times over the course of C8S3 aggregation. (b) Average photon arrival time over course of 3-hour aggregation.

Chapter 3: Summary

3.1 Conclusion

This work demonstrates how fiber-based dip probe integration with TCSPC enables *in situ* lifetime measurements that were previously inaccessible with conventional cuvette-based methods. By directly immersing the probe into chemical environments, this approach allows real-time monitoring of dynamic processes such as nanocrystal growth, dye aggregation, and morphological transitions without disrupting the native system. These results establish the dip probe as a versatile, durable method for probing excited-state dynamics across diverse dynamic material processes.

3.2 Future Directions

The optical route is currently aligned to a free space APD; ideally, a separate path will be implemented to include superconducting nanowire single photon detectors (SNSPDs) to enable detection of NIR-SWIR wavelength photon records. This will allow for a more confident replication of the HgTe quantum dot experiment with the SNSPDs because the current APDs are not suited for NIR measurements. Emission larger than 1000 nm in wavelength do not have enough energy to cross the silicon bandgap of 1.11 eV while the synthesis produces HgTe dots with emission from 915-1180 nm.[22,23]

It would also be ideal to utilize dual dip probes to measure both lifetimes and absorbance of the same sample during experiments. Connecting simultaneous lifetime and absorbance measurements would provide a more complete picture of excited-state processes by directly correlating structural and electronic evolution in real time. Together, the integration of NIR-SWIR detectors and dual-probe architectures represents a clear path for expanding the

capabilities of the dip probe method and pushing time-resolved spectroscopy toward broader applicability in photophysical monitoring of a chemical system.

References

(1) Wahl, M. *Time-Correlated Single Photon Counting*. PicoQuant GmbH.

(2) Lakowicz, J. R.; Masters, B. R. Principles of Fluorescence Spectroscopy, Third Edition. *J. Biomed. Opt.* **2008**, *13* (2), 029901. https://doi.org/10.1117/1.2904580.

(3) Cui, J.; Beyler, A. P.; Bischof, T. S.; Wilson, M. W. B.; Bawendi, M. G. Deconstructing the Photon Stream from Single Nanocrystals: From Binning to Correlation. *Chem. Soc. Rev.* **2014**, *43* (4), 1287–1310. https://doi.org/10.1039/C3CS60330J.

(4) *Jablonski Diagram | Perrin-Jablonski Diagram*. https://www.edinst.com/resource/what-is-a-jablonski-diagram-perrin-jablonski-diagram/ (accessed 2025-09-05).

(5) B&W Tek. *An Introduction to a Spectrometer - Fiber Optic Probes*. AZoM. https://www.azom.com/article.aspx?ArticleID=13373 (accessed 2025-09-10).

(6) An Optical Fiber-Based Spectrometer for Measurement of Fluorescence Lifetimes. *Microchem. J.* **1994**, *50* (3), 337–350. https://doi.org/10.1006/mchj.1994.1098.

(7) Saito Nogueira, M.; Cosci, A.; Teixeira Rosa, R. G.; Salvio, A. G.; Pratavieira, S.; Kurachi, C. Portable Fluorescence Lifetime Spectroscopy System for In-Situ Interrogation of Biological Tissues. *J. Biomed. Opt.* **2017**, *22* (12), 1–10. https://doi.org/10.1117/1.JBO.22.12.121608.

(8) Lagarto, J. L.; Shcheslavskiy, V.; Pavone, F. S.; Cicchi, R. Simultaneous Fluorescence Lifetime and Raman Fiber-Based Mapping of Tissues. *Opt. Lett.* **2020**, *45* (8), 2247–2250. https://doi.org/10.1364/OL.389300.

(9) Selanger, K. A.; Falnes, J.; Sikkeland, T. Fluorescence Lifetime Studies of Rhodamine 6G in Methanol. *J. Phys. Chem.* **1977**, *81* (20), 1960–1963. https://doi.org/10.1021/j100535a016.

(10) Bailey, A. D.; Deshmukh, A. P.; Bradbury, N. C.; Pengshung, M.; Atallah, T. L.; Williams, J. A.; Barotov, U.; Neuhauser, D.; Sletten, E. M.; Caram, J. R. Exploring the Design of Superradiant J-Aggregates from Amphiphilic Monomer Units. *Nanoscale* **2023**, *15* (8), 3841–3849. https://doi.org/10.1039/D2NR05747F.

(11) Ozin, G. A.; Arsenault, A.; Cademartiri, L. *Nanochemistry: A Chemical Approach to Nanomaterials*; 2008.

(12) *Exciton: An Introduction*. Ossila. https://www.ossila.com/pages/what-is-an-exciton (accessed 2025-09-05).

(13) Cotta, M. A. Quantum Dots and Their Applications: What Lies Ahead? *ACS Appl. Nano Mater.* **2020**, *3* (6), 4920–4924. https://doi.org/10.1021/acsanm.0c01386.

(14) Mousa Othman, D.; Weinstein, J.; Huang, N.; Ming, W.; Lyu, Q.; Hou, B. Solution-Processed Colloidal Quantum Dots for Internet of Things. *Nanoscale* **2024**, *16* (23), 10947–10974. https://doi.org/10.1039/D4NR00203B.

(15) Ma, S.; Du, S.; Pan, G.; Dai, S.; Xu, B.; Tian, W. Organic Molecular Aggregates: From Aggregation Structure to Emission Property. *Aggregate* **2021**, *2* (4), e96. https://doi.org/10.1002/agt2.96.

(16) Kasha, M.; Rawls, H. R.; Ashraf El-Bayoumi, M. The Exciton Model in Molecular Spectroscopy. *Pure Appl. Chem.* **1965**, *11* (3), 371–392. https://doi.org/10.1351/pac196511030371.

(17) Sebastian, E.; Philip, A. M.; Benny, A.; Hariharan, M. Null Exciton Splitting in Chromophoric Greek Cross (+) Aggregate. *Angew. Chem. Int. Ed.* **2018**, *57* (48), 15696–15701. https://doi.org/10.1002/anie.201810209.

(18) Prokhorov, V. V.; Prusakov, K. A.; Pozin, S. I.; Perelygina, O. M.; Mal'tsev, E. I.; Nekrasov, A. A. Crystallographic Models of Ribbons and Ribbon-Based J-Aggregate Nanotubes from the Geometry of Tube Ends. *Phys. Chem. Chem. Phys.* **2024**, *26* (45), 28650–28661. https://doi.org/10.1039/D4CP03559C.

(19) Liu, R. Unpublished.

(20) von Berlepsch, H.; Kirstein, S.; Hania, R.; Pugžlys, A.; Böttcher, C. Modification of the Nanoscale Structure of the J-Aggregate of a Sulfonate-Substituted Amphiphilic Carbocyanine Dye through Incorporation of Surface-Active Additives. *J. Phys. Chem. B* **2007**, *111* (7), 1701–1711. https://doi.org/10.1021/jp065826n.

(21) Megow, J.; Röhr, M.; Busch, M.; Renger, T.; Mitric, R.; Kirstein, S.; Rabe, J.; May, V. Site-Dependence of Van Der Waals Interaction Explains Exciton Spectra of Double-Walled Tubular J-Aggregates. *Phys Chem Chem Phys* **2015**, *17*, 6741–6747. https://doi.org/10.1039/C4CP05945J.

(22) Kittel, C. *Introduction to Solid State Physics*, 8. ed., [repr.].; Wiley: Hoboken, NJ, 20.

(23) Rinnerbauer, V.; Hingerl, K.; Kovalenko, M.; Heiss, W. Effect of Quantum Confinement on Higher Transitions in HgTe Nanocrystals. *Appl. Phys. Lett.* **2006**, *89* (19), 193114. https://doi.org/10.1063/1.2387110.